IEEE Access
Multidisciplinary | Rapid Review | Open Access Journal

Received August 27, 2018, accepted October 1, 2018, date of publication November 9, 2018, date of current version January 23, 2019.

Digital Object Identifier 10.1109/ACCESS.2018.2880224

Diagnosing Metabolic Syndrome Using Genetically Optimised Bayesian ARTMAP

HABEEBAH ADAMU KAKUDI[1,2], (Member, IEEE), CHU KIONG LOO[1], (Senior Member, IEEE), FOONG MING MOY[3], NAOKI MASUYAMA[4], (Member, IEEE), AND KITSUCHART PASUPA[5], (Senior Member, IEEE)

[1]Faculty of Computer Science and Information Technology, University of Malaya, Kuala Lumpur 50603, Malaysia
[2]Department of Computer Science, Faculty of Computer Science and Information Technology, Bayero University, Kano 3011, Nigeria
[3]Julius Centre University of Malaya, Department of Social and Preventive Medicine, Faculty of Medicine, University of Malaya, Kuala Lumpur 50603, Malaysia
[4]Department of Computer Science and Intelligent Systems, Graduate School of Engineering, Osaka Prefecture University, Osaka 599-8531, Japan
[5]Faculty of Information Technology, King Mongkut's Institute of Technology Ladkrabang, Bangkok 10520, Thailand

Corresponding authors: Kitsuchart Pasupa (kitsuchart@it.kmitl.ac.th) and Chu Kiong Loo (ckloo.um@um.edu.my)

This work was supported in part by the University of Malaya Postgraduate Research Fund under Project PG038-2016A, in part by the UM Grand Challenge Project under Project GC003A-14HTM, and in part by the Faculty of Information Technology, King Mongkut's Institute of Technology Ladkrabang.

ABSTRACT Metabolic Syndrome (MetS) constitutes of metabolic abnormalities that lead to non-communicable diseases, such as type II diabetes, cardiovascular diseases, and cancer. Early and accurate diagnosis of this abnormality is required to prevent its further progression to these diseases. This paper aims to diagnose the risk of MetS using a new non-clinical approach called "genetically optimized Bayesian adaptive resonance theory mapping" (GOBAM). We evolve the Bayesian adaptive resonance theory mapping (BAM) by using genetic algorithm to optimize the parameters of BAM and its training input sequence. We use the GOBAM algorithm to classify individuals as either being at risk of MetS or not at risk of MetS with a related posterior probability, which ranges between 0 and 1. A data set of 11 237 Malaysians from the CLUSTer study stratified by age and gender into four subcategories was used to evaluate the proposed GOBAM algorithm. The comparative evaluation of our results suggested that the GOBAM performs significantly better than other classical adaptive resonance theory mapping models on the area under the receiver operating characteristic curves (AUC) and others criteria. Our algorithm gives an AUC of 86.42 %, 87.04 %, 91.08 %, and 89.24 % for the young female, middle aged female, young male, and middle-aged male subcategories, respectively. The proposed model can be used to support medical practitioners in accurate and early diagnosis of MetS.

INDEX TERMS Metabolic syndrome, adaptive resonance theory, Bayesian ARTMAP, genetic algorithm.

I. INTRODUCTION

Metabolic syndrome (MetS) comprises metabolic abnormalities that are defined by abdominal obesity, dyslipidemia, hyperglycaemia, impaired glucose metabolism, and hypertension. It is characterized by two major non-communicable diseases (NCDs)–the cardiovascular disease (CVD) and type II diabetes mellitus (T2DM) [1]–[3]. Growing evidence shows MetS as a high predictive factor of developing CVD [4], [5] and T2DM [6]. MetS is also connected with the risk of other NCDs such as cancer, blood clotting, psychiatric disorders, polycystic ovary syndrome, and sub-clinical hypercortisolism [7].

MetS as a global pandemic is prevalent in Africa [8], [9], Europe [10], the United States [11], [12], and Asia [13]–[15]. Malaysia is not exempted from the global MetS pandemic. In fact, the prevalence of MetS in Malaysia is high compared with other Southeast Asian countries, where 32.1 to 42.5 % of Malaysians have been diagnosed with MetS [16]. Studies have also shown an average MetS prevalence 33.0 % in Malaysian Adults [17] and adolescents [18]. Thailand also has a high prevalence of MetS where 32.0 % of all Thai adults have MetS [19]. This has resulted in heightened levels of NCDs in Malaysians [20] and other Southeast Asians such as the Thais.

NCDs present themselves as a consequence of MetS and have the highest morbidity and mortality rate in Malaysia [21]. The global economic burden of MetS resulting from this high morbidity and mortality rate has increased

urgency for researches to address the associative risk factors–early detection, and diagnosis of MetS [22], [23]. The need for early diagnoses, management, and treatment of MetS cannot be overlooked due the significant health burden incurred [24].

The dichotomous approach is the traditional diagnosis of MetS using clinically approved binary diagnostic criteria. The most common definitions were proposed by the World Health Organization (WHO) [25], the National Cholesterol Education Program–Third Adult Treatment Panel (NCEP ATP III) [26], the International Diabetes Federation (IDF) [27], the European Category for the Study of Insulin Resistance (EGIR) [28], American Heart Association–National Heart, Lung, and Blood Institute (AHA/NHLBI) [29], and the Harmonized (Joint Interim Statement) definition [30]. These expert bodies determined the dichotomous diagnostic criteria for MetS which requires three or more of the following MetS risk factors:

- Waist Circumference (WC) $\geq$ 102 cm for men and WC $\geq$ 88 cm for women;
- Increased Triglyceride (TG) $\geq$ 150 mg/dl or being under treatment;
- Low, High-density Lipoprotein Cholesterol (HDL-C) $<$ 40 mg/dl for men and HDL-C $<$ 50 mg/dl for women or being under treatment;
- Elevated blood pressure, Systolic Blood Pressure (SBP) $\geq$ 130 mmHg, or Diastolic Blood Pressure (DBP) $\geq$ 85 mmHg or receiving anti-hypertensive medications;
- Increased Fasting Plasma Glucose (FPG) $\geq$ 100 mg/dl or treatment for hyperglycaemia.

Despite sharing common risk factors, the dichotomous approach varies in terms of relevance and positive predictive value resulting in the non-uniformity of these definitions. Additionally, dichotomizing the risk factors leads to information loss because MetS is predicted by isolating continuous MetS risk factors. The threshold cut-off point of the MetS risk factors for each of the dichotomous MetS definitions is population specific. This makes it difficult to apply the same definition evenly across different populations [31]. Furthermore, there are disparities in MetS diagnosis due to different definitions of MetS [32]. Currently, a standard recommendation for the specific treatment of MetS is unavailable. However, Ginsberg suggested that MetS can be treated by considering each compounding abnormality or components regardless of whether they occur in isolation or otherwise [33]. Since guidelines for MetS management recommends addressing each MetS risk abnormality in isolation, a diagnosis method which includes all the risk factors is required. In a bid to find a diagnostic measure of MetS which encompasses all the MetS risk factors, scholars have proposed the application of three main non-clinical methods. These non-clinical methods include statistical methods [34]–[49], mathematical quantification [50]–[53], and machine learning [54]–[59] techniques. A detailed review of these techniques will be presented in Section II.

This paper examines the potential of genetically optimizing the Bayesian Adaptive Resonance Theory Mapping (BAM) in order to diagnose the risk of MetS. The BAM is a combination of Fuzzy Adaptive Resonance Theory Mapping (FAM) with Bayesian learning. In the BAM, the hyper-rectangular category shape of the FAM is interchanged with Gaussian hypersphere category shapes, and the volume of the hypersphere has the ability to grow and shrink as categories are created. This flexibility afforded to the volume of the hypersphere reduces the creation of unnecessary categories. Thus, this makes the predictive performance of BAM better than the FAM. BAM applies Gaussian categories and replaces the competitive learning of FAM with Bayesian learning to train the input samples. The patterns in FAM are linked with the Gaussian categories while probabilistic inference is used to link the Gaussian spheres with classes to perform Adaptive Resonance Theory Mapping (ARTMAP) learning. However, the BAM is sensitive to parameter tuning and the order sample pattern sequence.

This paper proposes the Genetically Optimised Bayesian Adaptive Resonance Theory Mapping (GOBAM) for MetS diagnosis. In pursuing this objective, the proposed solution offers the following contributions:

1) We propose GOBAM which optimizes the parameters of BAM and training sample sequence using Genetic Algorithm (GA);
2) Generation of a probability value to measure the severity of the risk of MetS;
3) While comparisons of classifiers in current studies focus solely on predictive accuracy, the focus of this study is to improve their accuracy and generalization using different performance measures that are important to medical diagnostic tests, e.g. Area Under the Receiver Operating Characteristic Curve (AUC), sensitivity, specificity; and
4) A comprehensive analysis between GOBAM and three other types of Adaptive Resonance Theory (ART) models: FAM [60], BAM [61], and Genetic-FAM (GA-FAM) [62] for classification of MetS using a real-world sample dataset of 33,459 Malaysian participants partitioned into four categories according to gender and age.

As far as existing literature is concerned, no published articles diagnosed MetS using any kind of ART model.

II. LITERATURE REVIEW

This section briefly discusses the studies related to the different types of statistical, mathematical quantification, and machine learning techniques used to diagnose the risk of MetS. This is then followed by a description of the different types of ARTMAP networks and their progression to the BAM.

A. STATISTICAL TECHNIQUES

The statistical techniques proposed for the diagnosis of MetS include the Principal Component Analysis (PCA), z-score,

and Confirmatory Factor Analysis (CFA). All these statistical techniques are used to derive a value known as Continuous MetS (cMetS) score. The cMetS score represents the level of the risk of MetS based on the MetS risk factor measurement values. The z-score was the earliest statistical technique used to generate a cMetS score by Batey *et al.* [34] in 1997. The cMetS is computed using the z-score by taking the difference between the sample mean of each attribute and each sample value in the population, and dividing the result by the standard deviation of each attribute in the population [35], [36], [38], [43], [45]. The PCA operates by decreasing the dimensionality of the attributes of a dataset in order to make data more interpretable while preserving the relevant information [47]. Dimensionality reduction results in the output of principal components. In the context of MetS, the largest principal component derived from a PCA–which explains the maximum total variance of the all MetS risk factor values of a population–represents the cMetS score [37], [39], [41], [44], [46]. The PCA is also used to find relevant associations of risk factors with MetS [40]. CFA accounts for the common variance amongst attributes of a dataset. It is used to check how well the variables in a hypothesis fits in an existing model. The application of CFA in the diagnosis of MetS involves the selection of variables from prior MetS models which are used to compare between existing hypothesized MetS models. Studies have recorded the CFA in the developments of the cMetS score [42], [48], [49]. However, the statistical methods are sample specific, and the same model cannot be applied to different populations. Also, the impact of all the MetS risk factors is assumed to be equal leading to unaccountability in their different effects.

B. MATHEMATICAL FORMULATIONS

Mathematical formulations have also been applied to derive the risk of MetS. Jeong *et al.* [50] derived the Areal Similarity Degree (ASD) to quantify the risk of MetS in Koreans. The risk factors' weight is derived from eigenvector priority estimation. The weights provide a visual assessment of MetS using radar chart by using a single value ranging between 1 to 0. However, the performance measure of their formula was not evaluated. Therefore, the risk of MetS was quantified with weighting the risk factors in the ASD with weights obtained by Quantum Particle Swarm Optimization (QPSO) [52]. The performance of the ASD with QPSO was also evaluated with MediBoost, which is a machine learning technique [53]. Soldatovic and his colleagues also derived a risk quantification score called the ''siMS score'' [51]. The siMS score is compared across different populations. In comparison, the method proved to be superior to the Framingham risk score in the diagnosis of the risk of MetS.

C. MACHINE LEARNING TECHNIQUES

Machine learning techniques were widely used in the prediction of MetS. For example, Logistic Regression, Support Vector Machine, and Artificial Neural Network (ANN) were used to predict MetS in schizophrenic patients [58]. Biochemical parameters such as Homoeostatic Model Assessment-Insulin Resistance (HOMA-IR) and serum adiponectin were included in the MetS risk factors for the prediction of six-year incidence of MetS using ANN. The technique gave a sensitivity and specificity of 93.0 % and 91.0 %, respectively [54]. However, these risk factors are difficult to measure and may not be efficient in daily clinical practice. As an easy and low-cost identification method, ANN was used to predict MetS [63]. Romero-Saldana *et al.* [59] applied Decision Tree and Multiple Logistic Regression to predict MetS with accuracy, sensitivity and specificity of 94.2 %, 91.6 %, and 95.7 %, respectively. However, body fat mass, waist-to-height ratio, and waist-to-hip ratio included as part of the risk factors for the prediction of MetS in their work are not clinically recognized as risk factors of MetS. In another study, Fuzzy ANN was used to search for significant combinations of risk factors connected with MetS [55]. Furthermore, the association between the traditional MetS risk factors, human nuclear receptors responsible for regulating fatty acid storage and glucose metabolism, and environmental factors was investigated using Back-error Propagation ANN (BPANN) [64]. This study only sought to find associations of MetS with new risk factors.

In MetS diagnosis, predictive accuracy is the capacity of a diagnostic test to distinguish between individuals with or without MetS. Murguia-Romero *et al.* [56] used BPANN to predict MetS. They found that there was a threefold increase in the positive predictive value of using machine learning techniques to predict MetS than the current clinical dichotomous method. Also, in [53], the MediBoost outperformed the ASD with AUC, sensitivity and specificity of 99.38 %, 98.77 %, and 99.55 %, respectively. This further emphasizes the robustness of machine learning methods in the prediction and diagnosis of the risk of MetS. However, BPANN is a black box algorithm. Explicit information relating to the risk quantification of MetS that is required by both individuals and clinical practitioners is not available in the output of BPANN.

Adaptive Resosnance Theory (ART) was first proposed by Grossbert [65]. It is an incremental learning algorithm which leverages on the cognitive and neural ability of the brain to quickly learn, and recognize objects and patterns. ART learns in real time using unsupervised learning. The competency of ART to provide a solution to the stability-plasticity problem, i.e., the ability to learn new input patterns while remaining stable to insignificant patterns, prompted its supervised learning adaptation called the ARTMAP [66]. ARTMAP consists of two ART networks connected by an associative learning network and an inner controller that can carry out fast and stable incremental learning as a supervised learning system. The initial modification of the ART and ARTMAP networks are the Fuzzy ART (FA) [67] and FAM [60] algorithms.

FAM is an ART network integrated with Fuzzy logic which comprises of two ART networks, ART_a and ART_b related by an intermediary ART network, ART_m. ART_a and ART_b

are self-organizing ART networks that have stable category recognition. Learning creates hyper-rectangular categories where input patterns will be mapped to classes. However, these hyper-rectangular categories can only increase and are insensitive to the pattern of input data. FAM is sensitive to statistical overlapping between clusters [68], [69]. For the purpose of clarity, categories, and clusters will be used interchangeably in this paper. This problem results in the formation of a high number of pattern recognition clusters with the overlapping allocation of nodes referred to as category proliferation. Category proliferation creates an output neural network architecture consisting of a redundant number of categories which incurs a high computational and memory allocation cost with a reduction in classifier performance. ART with spatial and temporal evidence integration for dynamic predictive mapping, ART-EMAP [70], Gaussian ARTMAP [71], [72], PROBART [69], and ARTMAP-IC [72] are examples of FAM variants that have been proposed as solutions to the problem of category proliferation.

Progressively, a more successful approach to the problem associated with FAM was proposed as the Bayesian ART (BA) and BAM [61]. BA and BAM architecture is an integration of the Bayes' theorem into the ART and ARTMAP architecture, respectively. BAM is a neural network structure which estimates category and class probabilities with high prediction performance and computational efficiency [61]. It integrates the features of the FAM with Bayesian probability inference. Instead of the hyper-rectangular structure of categories in the FAM network, categories are represented as Gaussian hypersphere/hypervolume categories. The Gaussian function replaces the fuzzy set theory in the ARTMAP network thereby allowing for patterns which were wrongly allocated or stuck in the hyper-rectangular corners to be correctly placed in appropriate hypersphere categories. The Gaussian categories allow categories to increase and decrease by constraining the cluster hypervolume, and thus providing a well-defined representation of input patterns. The BAM classifies patterns using statistical learning and inference giving it more flexibility and adaptability. Class prediction depends on all the clusters that are statistically linked with the class rather than the hard category assignment based on the winning category in the FAM. Overall, a better generalization of pattern classification is realized by the learning and inference of the BAM network. However, the classification performance of the BAM depends on the choice of the optimal training input sequence and parameter settings. These two indicators are important because the choice of the training input sequence influences the selection of appropriate algorithm parameter settings. Therefore, these two tasks must be carried out simultaneously.

In this paper, we concentrate on the optimization of the BAM network for the diagnosis and prediction of MetS. This is because BAM is an incremental supervised learning algorithm consisting of both probabilistic inference and ART properties with minimal expected loss.

III. METHODOLOGY

A. BAM

Real time distributed data is represented using multidimensional Gaussian clusters in BA. These cluster are shaped as hyperspheres. Each sphere is parameterized with the mean of the sample data associated with the cluster, the covariance matrix, and a priori probability. The mean is the central mass of the Gaussian hypersphere, the covariance matrix defines its shape and the a priori probability represents its superiority over other clusters. There are three main stages in the BAM network, namely cluster selection, cluster pairing, and learning.

1) CLUSTER SELECTION

All current clusters are eligible to be selected during training phase. The j-th cluster of each D-dimensional sample x is represented by a posterior probability of category ω_j given x defined as follows,

$$P\left(\omega_j|x\right) = \frac{p\left(x|\omega_j\right)P(\omega_j)}{\sum_{n=1}^{N_C} p(x|\omega_n)P(\omega_n)}, \tag{1}$$

where x is the sample input, ω_j represents the j-th cluster. $P(\omega_j)$ is the assumed prior probability of the j-th cluster, defined as

$$P(\omega_j) = \frac{n_j}{\sum_{j=1}^{N_C} n_j}, \tag{2}$$

where N_C is the number of clusters and n_j represents the number of counts of training samples categorized into the cluster j. $p(x|\omega_j)$ represents the conditional probability density of x given cluster ω_j defined as

$$p(x|\omega_j) = \frac{1}{(2\pi)^{\frac{D}{2}}|\Sigma_j|^{\frac{1}{2}}} \exp\left[-\frac{1}{2}\left(x-\mu_j\right)^T \Sigma_j^{-1}\left(x-\hat{\mu}_j\right)\right], \tag{3}$$

where μ_j and Σ_j are the D-dimensional mean vector and $D \times D$ co-variance matrix of j-th cluster, respectively.

The cluster with the highest posterior probability is selected as the winning cluster G, computed as

$$G = \underset{j\in N_c}{arg\ max}\left(P\left(\omega_j|x\right)\right). \tag{4}$$

The robustness of the BA is enforced by selection of a winning, G cluster–ω_j that either has the largest value of the prior probability $p(\omega_j)$ or the cluster with the closest distance to the current sample input or both. The addition of the Bayes' theorem as another condition for selection also enables the accurate selection of a winning cluster.

2) CLUSTER MATCH (VIGILANCE TEST)

The vigilance test is carried out to constrain the size of the winning cluster, G. The test ensures that the volume of the Gaussian hypersphere G, V_G, does not exceed the maximum volume of a hypersphere, $V_{\max}$ for a winning cluster as follows:

$$V_G \leq V_{\max}. \tag{5}$$

where V_G is the determinant of the Gaussian covariance matrix, Σ_G is computed as the product of each dimensions' variances, σ as follows:

$$V_G \triangleq \det(\Sigma_G) = \prod_{i=1}^{d} \sigma_{G_d}^2. \tag{6}$$

If the vigilance test (5) is passed by the winning cluster, then match tracking criterion will be checked. However, if G fails the vigilance test, then it is removed from the current competition by setting its posterior probability with (1) to zero, and the search continues until a winning cluster that passes test is selected. If no cluster from the existing clusters passes the vigilance test then a new cluster is created with a hypervolume that meets (5).

3) MATCH TRACKING

In the map field of the BAM network, the class posterior probability is used to update the winning class category $P(y_i|G)$. A class posterior probability threshold, $P_{\min}$, is set as follows,

$$P(y_i|G) \geq P_{\min}, \tag{7}$$

such that if it is less than the class posterior probability, then the i-th class will be associated with the winning G category; $P(y_i|G)$ is derived from the BAM matrix $K = [N_{ij}]_{Y \times N_C}$, where Y is the number of classes, N_C is the number of clusters, and the ij-th input into the BAM matrix K, N_{ij} is the number of training input samples that are associated to the j-th cluster and belonging to the i-th class of the Y classes. $P(y_i|G)$ is calculated as

$$P(y_i|G) = \frac{N_{ij}}{\sum_{i=1}^{Y} \sum_{j=1}^{N_C} N_{ij}}, \tag{8}$$

where $i = 1, \ldots, Y$, and $j = 1, \ldots, N_C$. The full derivation of (8) using Bayes' theorem can be found in [61].

Match tracking will occur if $P(y_i|G)$ satisfies (7) and the winning cluster G will be associated with the class Y_i. However, if the match tracking criterion is not met, then match tracking is triggered by decreasing the maximum hypervolume, $V_{\max}$, by a small value δ as follows,

$$V_{\max,\text{new}} = V_G - \delta, \quad 0 < \delta \ll V_G. \tag{9}$$

$V_{\max,\text{new}}$ should be small enough to remove the current winning category V_G from the competition and initiate a search for a new winning cluster. The new winning cluster must have a new hypervolume that is less than $V_{\max}$ as in the vigilance test (5). This search iterates until the new winning category is found.

4) CLUSTER LEARNING

If the selected category G meets the vigilance test (5) and match tracking criterion (7) requirements, then the category parameters–mean vector μ_G and covariance matrix Σ_G–will be updated as follows:

$$\hat{\mu}_{G_{\text{new}}} = \frac{N_G}{N_G + 1} \hat{\mu}_{G_{\text{old}}} + \frac{1}{N_G + 1} x, \tag{10}$$

$$\hat{\Sigma}_{G_{\text{new}}} = \frac{N_G}{N_G + 1} \hat{\Sigma}_{G_{\text{old}}} + \frac{I}{N_G + 1} \left(x - \hat{\mu}_{G_{\text{new}}}\right) \times \left(x - \mu_{G_{\text{new}}}\right)^T, \tag{11}$$

where $N_G^{\text{new}} = N_G^{\text{old}} + 1$. N_G is the number of samples that are categorized by the G-th cluster and I is an identity matrix. Then the process will go back to cluster selection step explained in Section III-A.1 to learn the next input sample.

5) CLUSTER CREATION

A new cluster is created using

$$\begin{aligned} \hat{\mu}_{N_C} &= x \\ \hat{\Sigma}_{N_C} &= \eta (V_{\max})^{1/D} I \end{aligned} \tag{12}$$

such that the parameters of the cluster (10): the mean of the cluster $\hat{\mu}_{N_C}$ and the variance of the cluster $\hat{\Sigma}_{N_C}$ are initialized with the training input sample x, and $\eta (V_{\max})^{1/D} I$, where η is a small positive value and I is a $D \times D$ identity matrix, respectively.

6) INFERENCE IN BAM

Inference in the BAM network involves the use of all clusters associated to a class in order to define the class label during testing. Therefore, the class selected for a test sample x is defined as

$$y_i = \arg\max_i P(y_i|x) \tag{13}$$

where y_i is the class label for the test sample x and $P(y_i|x)$ is defined as

$$p(y_i|x) = \frac{\sum_{j=1}^{N_C} P(y_i|G) p(x|\omega_j) P(\omega_j)}{\sum_{i=1}^{Y} \sum_{j=1}^{N_C} P(y_i|G) P(x|\omega_j) P(\omega_j)} \tag{14}$$

where $P(y_i|G)$, $p(x|\omega_j)$, and $P(\omega_j)$ are defined in (8), (3), and (2), respectively.

The pseudo-code for the BAM algorithm is represented in algorithm 1. BAM has the advantage of solving the category proliferation problem by using Bayesian theory and probability to create and update the clusters. It achieves inference through the posterior probability. Clusters are illustrated as Gaussian hyper-volumes. However, the maximum hypervolume parameter, $V_{\max}$, of the BAM is sensitive to reiterative search that leads to high computational time and the creation of more clusters. These resulting clusters reduces the predictive performance of the BAM. Moreover, BAM is also sensitive to the sequence order of its input patterns. Therefore, these factors should be considered to get the optimal solution.

B. GENETIC ALGORITHM

GA is an optimization technique that is supported by the genetic and natural evolutionary concept of survival of the fittest. It is applied interchangeably with conventional heuristic search techniques. Candidate solution is referred to as populations, wherein the optimal solution is chosen after multiple iterative computations of each population's fitness value. The fitness value derived from the fitness function is an essential

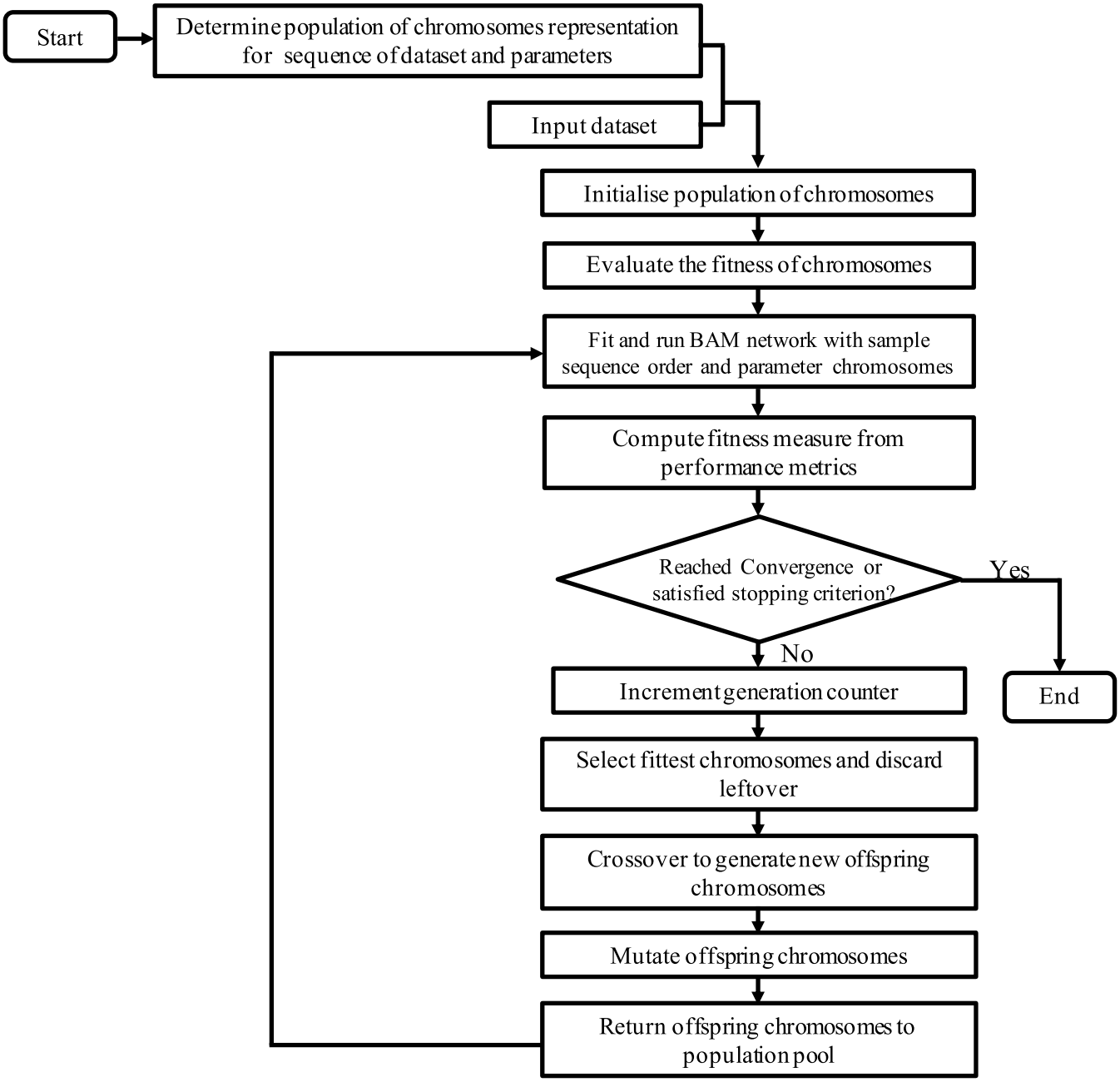

FIGURE 1. Flowchart of genetically optimized Bayesian ARTMAP.

parameter that determines the fitness of each chromosome. GA works by encoding complex structures of a population as a fixed length of binary strings, i.e., 2s and 3s, referred to as chromosomes. Populations in the GA, represented as chromosomes, are generated successively and alternately until the required solution is found. Searching is an exhaustive process of exploring and exploiting large search spaces resulting in a high chance of convergence without getting stuck in the local minima. The search process is conducted by population selection, recombination, and mutation. After that, chromosomes are ranked from the least-fit to the most-fit based on their fitness value. After that, chromosomes are ranked from the least-fit to the most-fit based on their fitness value. The selection produces a mating pool of equal-sized populations ($||P'||$, $||P||$) using selection techniques such as the roulette wheel selection. Only the superior chromosomes survive the selection process. Those survivors are referred to as the parents.

The major operations that affect the performance of a GA are crossover and mutation. In crossover, genes from the parent chromosomes are selected for reproduction based on the probability P_c (the *cross over probability* or *crossover*

Algorithm 1 BAM Algorithm

Require:
Samples: $A = (x_1, x_2, \ldots, x_N)$, where $x_N \in \Re^D$
Class label for each sample: y
Maximal hypervolume: $V_{\max}$
Vigilance parameter bias: δ_V
Match tracking class probability threshold: $P_{\min}$

Ensure: Class posterior probability $P(y_i|G)$ as in (7)

1: Input a vector x_N
2: **if** No clusters exist in ART network **then**
3: Create a new cluster as $N_{C_{\text{new}}}$ as in (12)
4: **else**
5: Compute a cluster posterior probability $P(\omega_j|x)$ as in (1)
6: Compute the index of winning cluster G as in (4)
7: Compute V_G as (6)
8: **if** $V_{G_k} \geq V_{\max}$ **then**
9: **if** All the categories do not pass the vigilance test **then**
10: Create a new category $N_{C_{\text{new}}}$ as in (12)
11: **else**
12: Remove y_G from selection and continue from Step 6 with the next chosen cluster
13: **end if**
14: **end if**
15: **end if**
16: Update the category frequency count N_{ij}
17: Compute the class posterior probability $P(y_i|G)$ as in (8)
18: **if** $P(y_i|G) \geq P_{\min}$ **then**
19: The map field learning takes place
20: Update $\hat{\mu}_{G,\text{new}}$ as in (10)
21: Update $\hat{\Sigma}_{G,\text{new}}$ as in (11)
22: **else**
23: **if** Match tracking fails with all categories **then**
24: Create a new category as $N_{C_{\text{new}}}$
25: **else**
26: Remove $\hat{\mu}_{G,\text{new}}$ from selection
27: Remove $\hat{\Sigma}_{G,\text{new}}$ from selection
28: Continue from Step 17 with a next candidate category
29: Update a maximal hypervolume $V_{\max}$ as in (9)
30: **end if**
31: **end if**
32: **if** $j < G$ **then**
33: Continue from Step 1 with $j \leftarrow j + 1$
34: **end if**

rate) between two selected individuals. The crossover operator selects genes from each chromosome and creates a new offspring. This is a random mechanism for exchanging genes using the one-point crossover, two-point crossover or homologue crossover. Enough chromosomes are generated to replace the discarded chromosomes. Thus, constancy in the number of chromosomes is ensured after each iteration. The mutation operator then subtly alters the genes codes of the new off-springs by randomly exchanging 0s with 1s or vice versa. Fitness values are evaluated for the offsprings and the mutated chromosomes, and this process is repeated. Mutation prevents all solutions in a population from falling into a local optimum.

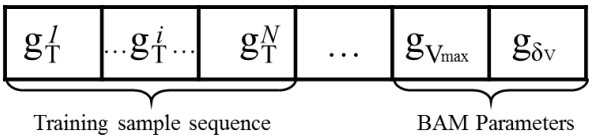

FIGURE 2. Chromosome representation.

IV. GENETICALLY OPTIMISED BAYESIAN ARTMAP (GOBAM)

GA can enable rapid convergence and a reduction of generalization errors in classifiers. Parameter optimization has been proposed to tackle problems associated with FAM using various evolutionary computation techniques [73]–[76]. However, to the best of our knowledge, no one has attempted to optimize the parameter settings and order of input sequence in the BAM neural network for medical diagnosis. Therefore, we propose GOBAM to diagnose MetS. As previously mentioned, a biased training sequence and under-tuned parameters affects the BAM's classification performance and its stability. Here, we utilize GA to search for an optimal combination of parameter values and training sample sequence in order to increase the predictive performance of BAM. The GOBAM algorithm is described in algorithm 2 and its flowchart in Fig. 1. There are two parameters that affect the performance of BAM, i.e., (i) maximal hypervolume: $V_{\max}$, (ii) vigilance parameter bias: δ_V.

A. CHROMOSOME DESIGN

The sequence of training sample and parameter settings of the BAM network will be optimized using GA. The illustration in Fig. 2 is a representation each chromosome in the search space.

Each chromosome g contains the followings:

1) The training sample sequence, $g_T^1 \sim g_T^N$, where N is the total number of training sample. $g_T^1 \sim g_T^N$ is encoded using permutation encoding. Each element of this chromosome subset must be a unique element representing the index of a training sample input.
2) The maximum hypervolume $g_{V_{\max}}$ which is encoded using real values ranging between [0] and [100].
3) The vigilance parameter bias, g_{δ_V}, represents the values of parameters δ_V.

Ten population of chromosomes $g(pop)$, $pop = 1, \ldots, 10$, are randomly initialized as possible candidate solutions. The sequence numbers of the training samples are randomly

Algorithm 2 GOBAM Algorithm

Require:
Samples: $[(x_1, y_1), (x_2, y_2), \ldots, (x_N, y_N)]$, $x_N \in \Re^D$
Training sample sequence chromosome: $g_T^1 \sim g_T^N$
Maximum hypervolume chromosome: $g_{V_{\max}}$
Vigilance parameter bias chromosome: g_{δ_V}
Size of the population: *pop*
Maximum number of generations: *maxGen*

Ensure: the best chromosome g_{best} from the population $g(pop)$

1: Initialize individual chromosomes $g_T^1 \sim g_T^n$, $g_{V_{\max}}$, g_{δ_V} in population $g(pop)$
2: Evaluate the fitness f_{AUC} of each chromosome in population $g(pop)$
3: **while** maximum iteration *iter* is not reached **or** convergence is not reached **do**
4: **for** $i = 1$ to *maxGen* **do**
5: Perform k-fold cross-validation of BAM
6: Calculate fitness f_{AUC} for each chromosome g
7: **end for**
8: **if** Convergence occurs **then**
9: Return best chromosomes g_{best}
10: **else**
11: Select the best pair of chromosomes based on the value of fitness function f_{AUC}
12: Perform crossover and mutation as described in Section IV-A to obtain new chromosomes g_{new}
13: **else**
14: Increase selection value to include optimum solutions
15: Decrease mutation value to converge onto solutions
16: **end if**
17: Update population $g(pop)$ with new chromosomes g_{new}
18: Update count *iter*
19: **end while**

ordered along with the values of the BAM parameters. The initialized chromosomes are passed into the BAM network for training and testing.

B. FITNESS EVALUATION

Next, GOBAM evaluates the fitness of each candidate solution in the BAM network and determines its fitness values using the fitness function. Our proposed algorithm is driven by the fitness function which enables the GA's search for optimal parameters and sequence of input patterns for the BAM. The fitness evaluation of the proposed GOBAM algorithm uses the AUC instead of accuracy because accuracy measures performance in relation to the total number of only the correct predictions while AUC is a summary measure of accuracy derived from the Receiver Operating Characteristic (ROC) curve which encompasses the sensitivity and specificity of the algorithm. The AUC is the estimated trapezoidal integration calculated in (15) as follow [77]:

$$f_{AUC} = \sum_{\varphi} \left\{ [s_\varphi \cdot \Delta(1-t)] + \frac{1}{2}[\Delta s \cdot \Delta(1-t)] \right\} \quad (15)$$

where $\Delta(1-t) = (1-t)_\varphi - (1-t)_{\varphi-1}$, $\Delta s = s_\varphi - s_{\varphi-1}$, and φ is an index.

C. SELECTION

The two parent individuals use the roulette wheel selection process. In the roulette process, chromosomes with the best fitness relative to the fitness values of the other chromosomes in the population have a higher chance of being selected. The selected parent chromosomes will be used to create new chromosomes using the GA operations–crossover and mutation.

D. CROSSOVER AND MUTATION

Crossover and mutation for the order of sample sequence and the BAM parameters are carried out differently because of the difference in the encoding process.

As depicted in Fig. 3, partially mapped crossover (PMX) [78] technique is applied for generating the offspring of the sequence order chromosome $g_T^1 \sim g_T^N$ in order to get the sequence order with the best fitness value. This technique is chosen because it does not allow for tie ranks in the offspring chromosome. After crossover, each element in the offspring chromosomes has to be a unique entry as is required in the sequence order of the training sample of the BAM network. Given two selected parents, Parent *A* and Parent *B*, PMX generates two offspring chromosomes, Offspring *A* and Offspring *B*, by uniformly selecting two random points in each of the parent chromosomes and swapping the elements within the bounds of those points. Each element in Parent *A* is mapped to the element in the same position in Parent *B*. Subsequently, the remaining blank fields in Offspring *A* are filled with elements from Parent *A*. However, if the element to be copied from Parent *A* to Offspring *A* is already present in Offspring *A*, then that element from Parent *A* will be exchanged with the element from Parent *B* which is mapped to the element in Parent *A*. This pattern continues until all the blank chromosome fields in Offspring *A* have been filled. Then the blank fields in Offspring *B* will be filled in by elements in Parent *B* not already present in Offspring *B* in the same order. Fig. 3 illustrates the crossover and mutation process of generating an offspring chromosome. Mutation is then carried out by randomly swapping two elements of each offspring chromosome.

The single point crossover is applied to the BAM parameter which is encoded as a real valued number. As shown in Fig. 3, this crossover technique generates offspring chromosomes by selecting one crossover point and swapping all the elements from that point between the parent chromosomes. The mutation of the BAM parameter offspring chromosome involves the addition and subtraction of some random float numbers.

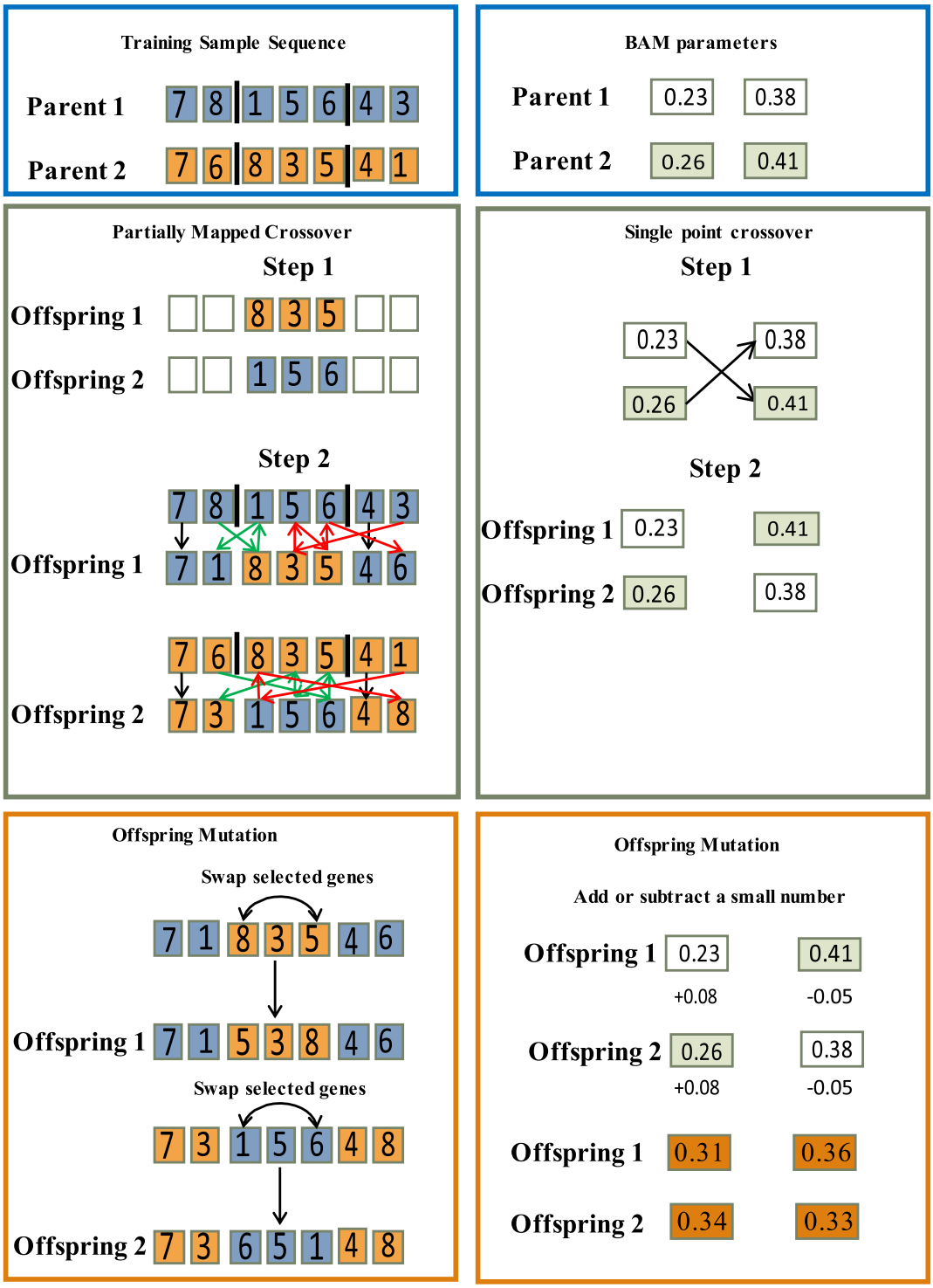

FIGURE 3. Chromosome crossover and mutation of the training sequence and BAM parameters.

V. EXPERIMENTS

A. MATERIALS

The dataset used in this study was compiled from the Clustering of Lifestyle risk factors and Understanding its association with stress on health and well-being among school Teachers in Malaysia (CLUSTer) study from March 2013 to March 2014 [79]. The University Malaya Medical Center (UMMC) ethic committee provided the approval to conduct the CLUSTer study. At baseline 11,237 teachers aged 20 to 69 years were selected via sampling of six out of the 12 Malaysian states. Schools qualified for the study were ranked based on the statistics of primary and secondary

TABLE 1. Characteristics of CLUSTer dataset [79]. Values are *n* (%) or mean ± standard deviation with minimum value (Mn) and maximum value (Mx). Diabetes mellitus case is identified when fasting blood glucose ≥ 5.5 (mmol/L) and/or physician diagnosed diabetes mellitus. Hypertension case is identified when Systolic BP ≥ 130 mm Hg and / or diastolic BP ≥ 85 mm Hg and / or physician diagnosed hypertension.

	Male		Female	
Number of Subjects, n (%)	2,133 (19.00)		9,104 (81.00)	
Age, years	44.33±9.43		42.95±8.40	
20–39 (young)	1,397 (19.71)		3,410 (82.25)	
40–64 (middle-aged)	736 (17.75)		5,691 (80.29)	
65 and above (old)	0		3	
Body Mass Index (kg/m^2)	44.43±7.45	Mn 23.9 Mx 81.7	40.38±7.78	Mn 19.3 Mx 100.0
Fasting Glucose (mmol/L)	5.00±0.58	Mn 3.1 Mx 7.6	4.82±0.50	Mn 3.1 Mx 7.1
Waist Circumference (cm)	89.55±10.99	Mn 57.0 Mx 137.0	79.68±10.69	Mn 48.0 Mx 121.0
HDL-Cholesterol (mmol/L)	1.24±0.26	Mn 0.52 Mx 2.3	1.49±0.34	Mn 0.5 Mx 3.0
Triglyceride (mmol/L)	1.56±0.77	Mn 0.6 Mx 5.0	1.12±0.48	Mn 0.6 Mx 3.3
Systolic Blood Pressure (mm Hg)	132.37±15.13	Mn 76.0 Mx 200.0	123.43±16.51	Mn 65.0 Mx 198.0
Diastolic Blood Pressure (mm Hg)	81.64±10.66	Mn 48.0 Mx 124.0	75.15±10.97	Mn 41.0 Mx 121.0
Diabetes mellitus n (%)	0		0	
Hypertension n (%)	182 (8.50)		454 (5.00)	

schools from the Ministry of Education, Malaysia for the year 2013. Participants were asked to answer a questionnaire and also engage in the required health screening procedures.

B. CLINICAL AND LABORATORY ASSESSMENTS

Measurement of WC was taken from the umbilicus, between the rib margin and the iliac crest at the end of normal expiration using non-elastic tape. SBP and DBP measurement were taken by a calibrated oscillometric sphygmomanometer on the left arm after a little rest.

Blood samples used to measure FPG total cholesterol, HDL-C, and TG was drawn from all the study participants after overnight fasting of 12–14 hours. These tests were measured as in-vitro diagnostic tests. The characteristics of the dataset are shown in Table 1.

C. IMPLEMENTATION

We implemented the proposed GOBAM algorithm in Matlab R2014a (8.3.0.532) on an Intel(R) Core(TM) i5-4200U CPU @ 1.6GHz 64-bit computer with 8.00 GB RAM. The algorithm was compared to standard ARTMAP algorithms such as FA, BAM, and GA-FAM on the CLUSTer [79] dataset as shown in Table 1. The age of participants was classified into six subject categories by gender and by age categories: young (between 20 and 39 years), middle-aged (between 40 and 64 years), and old (exceeding 65 years). There were no male participants over the age of 65 and only three female participants were identified. Therefore, only four categories of datasets will be used for the training and evaluation of our proposed GOBAM model–Young Male, Middle-age Male, Young Female, and Middle-age Female.

Due to the different scales of the risk factor measurements, it was necessary to normalize the input data to fit into a new range from 0 to 1 as follows:

$$x_{i_{new}} = \frac{x_i - x_{i_{\min}}}{x_{i_{\max}} - x_{i_{\min}}}. \tag{16}$$

where x_i is the i-th metabolic syndrome risk factor, $x_{i_{new}}$ is the new normalized input value, and $x_{i_{\max}}$ and $x_{i_{\min}}$ are the maximum and minimum values, respectively.

We used the 10-fold cross validation technique [80] to calculate the classification performance measures of our model. The results were averaged over 10 trials of 10-fold cross validation on each data set, while recording the balanced crossed validation performance measure on the hold-out test fold. The number of generations was set to 50. This is to reduce the bias of random sampling from the training dataset. Two different criteria were applied to terminate the training: (i) training was stopped if the mutation operator value is less than 0.01 and (ii) the training was stopped if the selection operator value was greater than 0.9.

D. PERFORMANCE EVALUATION METHODS

For machine learning classifiers where the problem requires a binary decision solution, as is the case for the MetS diagnosis in this paper, the performance of classifiers is evaluated using performance metrics known as predictive biomarkers [81]: accuracy, AUC, sensitivity, specificity, precision or positive predictive value (PPV), and negative predictive value (NPV). These quantitative performance metrics are derived using the metric values from the confusion matrix in Table 2. The confusion matrix shows the comparison between each predicted class with its actual class in four types of metrics values:

- True positives (*TP*) is the count of actual people with MetS correctly classified as having MetS.

TABLE 2. Calculation of sensitivity and specificity for a specific cut-off point of the predicted probability *P*: true positive (*TP*), false positive (*FP*), false negative (*FN*), and true negative (*TN*).

		Actual		
		MetS	Non-MetS	Total cases
Predicted	MetS	TP	FP	$TP+FP$
	Non-MetS	FN	TN	$FN+TN$
	Total cases	$TP+FN$	$FP+TN$	

- True negatives (TN) is the count of actual people without MetS correctly classified as not having MetS.
- False positives (FP) is the count of actual people with MetS incorrectly classified as not having MetS.
- False negatives (FN) is the count of actual people without MetS incorrectly classified as having MetS.

Note that the actual classification of MetS is based on any of the clinical definition of MetS such as the NCEP ATP III [26].

Below are the formulas for the various performance evaluation methods

1) ACCURACY

Accuracy is the ability of a classifier to accurately diagnose a disease.

$$Accuracy = \frac{(TP+TN)}{(TP+FP+FN+TN)} \times 100 \tag{17}$$

2) SENSITIVITY

Sensitivity is the ability of a classifier to correctly diagnose diseases amongst all actual disease classes.

$$Sensitivity = \frac{TP}{(TP+FN)} \times 100 \tag{18}$$

3) SPECIFICITY

Specificity is the ability of a classifier to correctly diagnose non-diseased amongst all actual non-diseased classes.

$$Specificity = \frac{TN}{(FP+TN)} \times 100 \tag{19}$$

4) POSITIVE PREDICTIVE VALUE

PPV is the probability that people classified by the model as having the disease actually have the disease.

$$PPV = \frac{TP}{(FP+TP)} \times 100 \tag{20}$$

5) NEGATIVE PREDICTIVE VALUE

NPV measure is the probability that the people classified as not having the disease actually do not have the disease.

$$NPV = \frac{TN}{(FN+TN)} \times 100 \tag{21}$$

6) RECEIVER OPERATING CHARACTERISTIC CURVE

The ROC curve captures the performance of the diagnosis system over the entire range of sensitivity and specificity values [82]. It is a two-dimensional plot which compares the performance of different diagnostic methods by visualizing their classification performances across different cut-off points. The confusion matrix consists of two class classifications: positive class (+1) and negative class (−1). It is plotted with sensitivity (18) on the y-axis and the 1-Specificity (19) values on the x-axis as a curve which lies between 0.5 and 1 with a value close to 1 indicating a very reliable classifier.

7) FRIEDMAN TEST

The Friedman test is a non-parametric test that ranks a performance measure of multiple algorithms for each data set separately [83]. The algorithm with the best performance measure is ranked highest, followed by the second best in rank and so on. In the case where algorithms are tied, an average ranks are assigned.

VI. EXPERIMENTAL RESULTS

In this section, we present experimental results to assess the performance of the proposed GOBAM method, and compare it with the classical ARTMAP algorithms–FAM, BAM, GA-FAM. The classification results are presented in Table 3 based on the four subcategories dataset–young male, middle-aged male, young female, and middle-aged female. The table shows the results of the number of categories generated, classification accuracy, AUC, sensitivity, specificity, positive and negative predictive value generated over 10-fold cross validation. The highest values are presented in bold face for each performance measure in the table. The AUC, accuracy, sensitivity, and PPV values of the GOBAM were higher than the other classic ARTMAP models for all the sub category datasets. This result confirms the superiority of the GOBAM model over the other ARTMAP models compared.

The ROC curves comparing the GOBAM, FAM, BAM, and GA-FAM models for the young male, middle-aged male, young female and middle-aged female are presented in Figs. 4a, 4b, 4c, and 4d, respectively. The AUC values of the GOBAM model were 85.85 %, 86.85 %, 90.89 %, and 88.10 % for young male, middle-aged male, young female, and middle-aged female sub category datasets, respectively.

Table 4 shows the results of the Friedman statistical test for comparing the proposed GOBAM model with the FAM, BAM, and GA-FAM models. The results of the eight subcategories for all the performance measures presented in Table 3 are averaged and ranked using the Friedman statistical test. The Friedman test ranks the performance measures in ascending order with the largest number representing the highest performance measure. The ranking of the proposed GOBAM model is 4.0, 3.0, 4.0, 1.5, 4.0 and 1.75 for AUC, accuracy, sensitivity, specificity, PPV, and NPV, respectively. The ranking of the Friedman statistical test shown in Table 4 revealed that the AUC ($p < 0.002$), accuracy ($p < 0.001$), sensitivity ($p < 0.001$), and PPV ($p < 0.02$) values of the proposed GOBAM model ranked significantly higher than the FAM, BAM, and GA-BAM models. This further reiterates the higher performance of the GOBAM model over the compared ARTMAP models.

TABLE 3. Performance comparison of the categorized datasets of FAM, BAM, GA-FAM, and GOBAM models (averaged over 10 trials of 10-fold cross-validation). For each model, the mean ± standard deviation are shown.

Data Sets	ARTMAP algorithms	Number of Clusters	AUC	Accuracy	Sensitivity	Specificity	PPV	NPV
Young Male	FAM [60]	31.7 ± 1.42	74.57 ± 0.04	72.47 ± 0.26	55.62 ± 0.08	80.79 ± 0.29	57.8 ± 0.23	**84.99 ± 0.06**
	BAM [61]	5.0 ± 0.85	82.68 ± 0.05	89.67 ± 0.03	94.98 ± 0.04	70.38 ± 0.11	92.19 ± 0.03	81.01 ± 0.12
	GAFAM [62]	12.4 ± 0.97	75.59 ± 0.05	79.06 ± 0.05	51.1 ± 0.05	**90.56 ± 0.05**	69.2 ± 0.12	81.98 ± 0.07
	GOBAM	5.0 ± 2.05	**85.85 ± 0.07**	**90.95 ± 0.04**	**95.33 ± 0.07**	76.38 ± 0.14	**93.28 ± 0.05**	81.6 ± 0.06
Middle-Aged Male	FAM [60]	54.6 ± 3.14	72.77 ± 0.05	74.67 ± 0.05	62.95 ± 0.09	82.45 ± 0.04	66.89 ± 0.1	78.66 ± 0.09
	BAM [61]	6.0 ± 0.83	85.32 ± 0.04	87.04 ± 0.03	81.73 ± 0.06	**89.82 ± 0.03**	79.96 ± 0.05	**90.68 ± 0.04**
	GAFAM [62]	38.1 ± 3.58	76.4 ± 0.05	76.93 ± 0.06	65.13 ± 0.05	85.93 ± 0.05	74.59 ± 0.1	78.2 ± 0.1
	GOBAM	6.0 ± 0.74	**86.85 ± 0.04**	**88.36 ± 0.03**	**91.51 ± 0.04**	82.19 ± 0.07	**91.07 ± 0.03**	83.49 ± 0.08
Young Female	FAM [60]	72.5 ± 3.44	81.55 ± 0.05	63.64 ± 0.44	51.17 ± 0.23	67.17 ± 0.47	48.08 ± 0.34	82.01 ± 0.34
	BAM [61]	5.0 ± 1.27	85.95 ± 0.04	**95.02 ± 0.01**	80.55 ± 0.06	**96.78 ± 0.01**	74.24 ± 0.08	**97.66 ± 0.01**
	GAFAM [62]	19.3 ± 2.01	81.39 ± 0.05	89.62 ± 0.02	53.37 ± 0.05	96.16 ± 0.02	70.76 ± 0.1	92.03 ± 0.03
	GOBAM	3.0 ± 0.0	**90.89 ± 0.03**	93.79 ± 0.02	**94.6 ± 0.03**	87.19 ± 0.04	**98.36 ± 0.01**	67.1 ± 0.09
Middle-aged Female	FAM [60]	125.7 ± 8.39	78.07 ± 0.05	74.44 ± 0.27	58.8 ± 0.08	81.94 ± 0.29	61.97 ± 0.23	86.5 ± 0.04
	BAM [61]	8.0 ± 1.43	87.72 ± 0.04	91.43 ± 0.02	79.61 ± 0.06	**94.85 ± 0.02**	81.2 ± 0.07	**94.23 ± 0.02**
	GAFAM [62]	53.5 ± 3.25	78.93 ± 0.04	82.65 ± 0.03	57.96 ± 0.04	91.92 ± 0.02	72.44 ± 0.07	85.43 ± 0.04
	GOBAM	9.0 ± 2.59	**88.10 ± 0.03**	**92.39 ± 0.02**	**95.67 ± 0.03**	80.53 ± 0.04	**94.69 ± 0.02**	83.71 ± 0.05

TABLE 4. Ranking of performance measures averaged over all the datasets using the Friedman statistical test.

	AUC	Accuracy	Sensitivity	Specificity	PPV	NPV
FAM [60]	1.25	1	1.5	2	1	2.75
BAM [61]	3	**3.25**	3	**3.25**	3	**3.25**
GAFAM [62]	1.75	2.75	1.5	**3.25**	2	2.25
GOBAM	**4**	3	**4**	1.5	**4**	1.75

However, the test ranked low in specificity ($p < 0.001$) and NPV ($p < 0.001$) values. Low specificity means the ability of GOBAM to identify individuals without MetS according to the JIS definition is low. Invariably, this means GOBAM is able to identify individuals with risk factor measurements that are close to the threshold as having MetS.

VII. DISCUSSION

The sensitivity of the ART networks towards the number of input samples and the order of input optimizing the BAM causes instability in category generation. In this paper, GA is applied to optimize the BAM parameter and the order of input sequence has stabilized the categories generation leading to the higher predictive performance measures in Table 3.

It is clear from the results that the proposed GOBAM model outperforms all the other classical ARTMAP algorithms in four measures–AUC, accuracy, sensitivity, and positive predictive value–for all the subcategories. However, the proposed GOBAM model had lesser specificity and NPV values. MetS is not considered as a disease but an abnormality which may lead to fatal diseases [30]. Since the NPV is the probability of the subject not actually being at risk of MetS, a misclassification is acceptable and will not be fatal to individuals. In fact, a low NPV and specificity can be a motivating factor for individuals to change towards a more positive lifestyle like healthy diet and increased exercise which can further reduce the risk of MetS [84].

Specificity of model tests how well individuals are actually classified as being negative. As sensitivity of a model increases, its specificity is reduced [85]. A highly specific model rules out the risk of MetS if the sample is positive. Once again, in the case of MetS, a low specificity value is not an indication of low predictive performance. The fact that an individual is diagnosed as being at risk of MetS even though he is not at risk will motivate him toward a healthier lifestyle. This diagnosis is helpful to individuals because the proposed GOBAM is less specific and has wider applicability in the management of MetS.

In this paper, we focus on the diagnosis of MetS for Malaysians especially in people with borderline measurement values. MetS is a lifestyle abnormality and not a disease [2]. Therefore, emphasis should be not only on accurately diagnosing those individuals with the abnormality but also individuals at risk of having the abnormality in the near future, i.e., those with borderline MetS risk factor measurements. From the results of the GOBAM, consideration should be given to the false positive metric in this respect.

The proposed GOBAM model outputs a posterior probability that is associated with the class category of an input. The probability value which ranges from 0 to 1 is a value which indicates the level of classification of the model on a particular input sample. The posterior probability value can be effectively used in clinical applications of MetS. For example, let us assume that a middle-aged male presents with a BMI of 28 kg/m^2 and MetS risk factor measurement values as shown in Table 5. According to the JIS [30] definition, he will not be diagnosed as being at risk of MetS (See Section I). However, his risk factor measurement values have exceeded the threshold of fasting glucose and are at borderline in waist circumference, HDL-Cholesterol overweight,

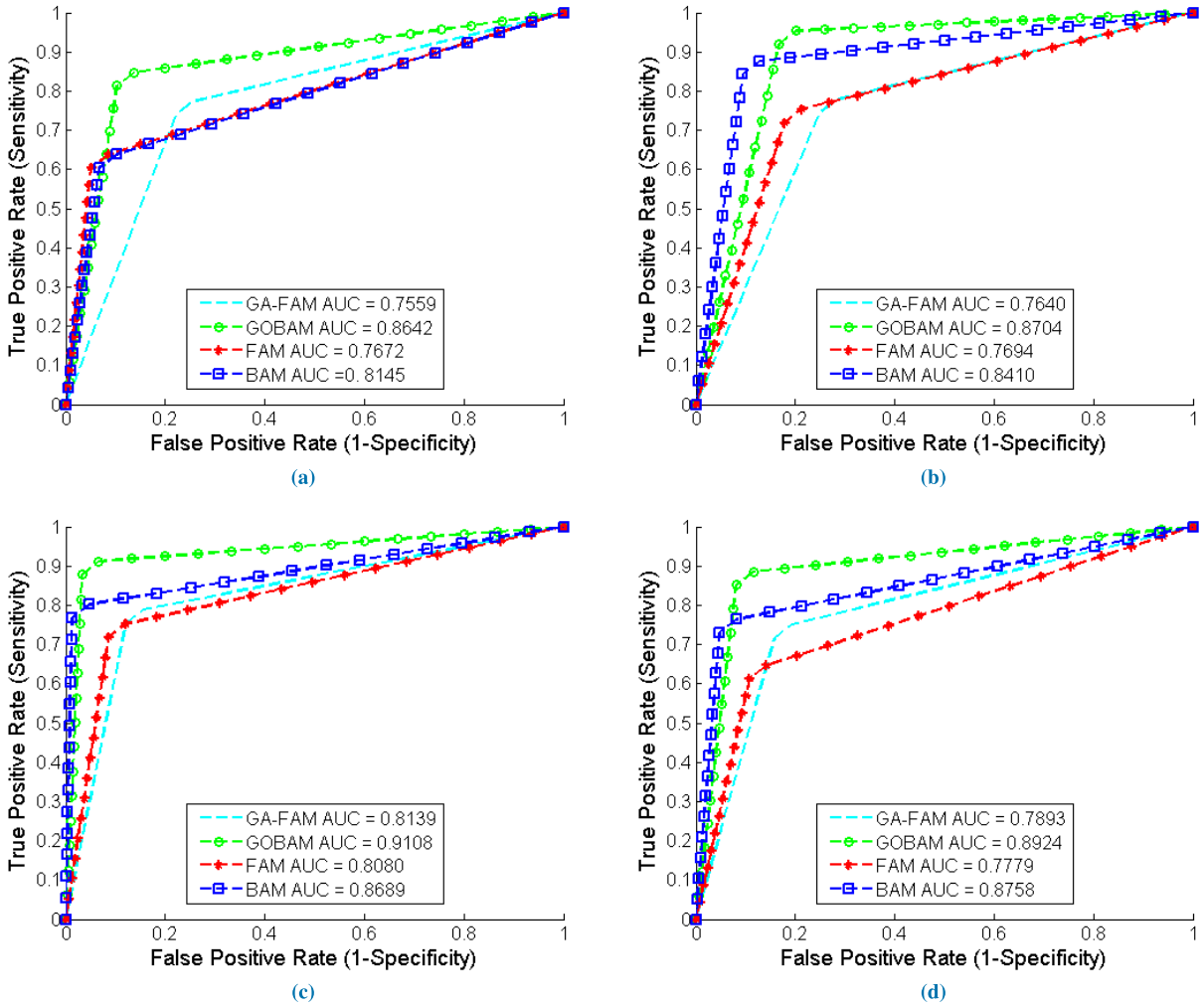

FIGURE 4. ROC curves and AUC values comparing GOBAM and classic ARTMAP models for the four data set subcategories. (a) Young male. (b) Middle-aged male. (c) Young female. (d) Middle-aged female.

and blood pressure threshold risk factor values. To identify these risks, GOBAM generates probability estimations for each class prediction which can aid in ranking an individual with borderline values. After running this sample through our proposed GOBAM model, this middle aged male is classified as having MetS with 0.8367 posterior probability. This result could assist medical practitioners to provide support and management to their patients at an early stage before the increase in the risk of MetS.

By optimizing the parameters and sequence of input, the proposed GOBAM model obtains better performance on accuracy, AUC, and sensitivity. Our proposed model supports the diagnostic decision of medical practitioners by giving them a labeled diagnosis of the risk of MetS. Early knowledge of the risk of MetS especially in patients who present with borderline measurement values will be of assistance in clinical practice. Both the patients and their medical practitioners will be aware of the risk of the abnormality and can chart out preventive and management solutions to prevent further progression. Furthermore, the burden of cost associated diseases such as T2DM, CVD, and cancer [86] resulting from the presence of MetS will be greatly reduced. Additionally, emotional burdens such as depression, oxidative stress and distress have been known to be associated with the presence of MetS and its associated diseases [87]–[89]. Health and lifestyle management such as dietary management [90] and increased physical exercise [91] can be used to reduce the risk of MetS and its progression. Early awareness of the risk of MetS obtained from our proposed model will assist in designing individualized clinical and personalized health management systems of MetS.

This study has the following limitations. First, the cohort study for the dataset used was restricted to Malaysians school teachers. Secondly, the incidence of MetS was low in the dataset, hence the low rate of true positive predictions. This bias was decreased by performing the 10-fold cross validation and averaging the results. Moreover, results from the other classic ARTMAP algorithms are similar to the results from

TABLE 5. MetS measurements of a Male Individual according to the dichotomous method.

MetS Risk Factor	Measurement	JIS threshold	JIS MetS Assessment
Fasting Blood Glucose	6.0 mmol/L	$>$ 5.6 mmol/L	Yes
Waist Circumference	101 cm	$>$ 102 cm	No
HDL−Cholesterol	1.1 mmol/L	$<$ 1.0 mmol/L	Yes
Triglyceride	1.2 mmol/L	$>$ 1.7 mmol/L	No
Systolic Blood Pressure	129 mm Hg	$>$ 130 mm Hg	No
Diastolic Blood Pressure	80 mm Hg	$>$ 85 mmHg	No

the proposed GOBAM algorithm. This further ensures the robustness of the results obtained.

VIII. CONCLUSION

In this work, a new approach for MetS diagnosis is explored by genetically optimizing the hypervolume parameter of the BAM and its sequence of training input samples to build a model for the diagnosis of the risk of MetS. The purpose of applying and investigating this approach is to improve the predictive performance of the BAM to diagnose the risk of MetS in relation to age and gender. The predictive performance of the proposed GOBAM was evaluated using results generated from a 10-fold cross validation process on CLUSTer dataset of Malaysians stratified according to age and gender. The proposed GOBAM model was compared with FAM, BAM, and GA-FAM based on the AUC, accuracy, sensitivity, specificity, PPV, and NPV.

The goal of this work is to develop an intelligent model which will assist clinical practitioners in improving the quality of life of their patients. The results of our proposed model will reduce the risk of MetS which could lead to fatal diseases such as the T2DM and CVD. We have also illustrated the practical applicability of the proposed GOBAM model in the clinical practice of MetS diagnosis. Our proposed GOBAM model generates a probability value as an indication of how well a patient is classified as being at risk of MetS. The proposed model enables the early diagnosis of the risk of MetS at a stage where treatment and management are more effective. This will help to reduce the progression of MetS which may result in actual diseases such as T2DM and cardiovascular diseases.

Considering the rapid increase in the prevalence of MetS annually [14], a perceptive intelligent diagnosis mechanism has been developed to support the diagnosis of the risk of MetS with a probability value. Therefore, our proposed model is timely for the intervention of the risk of MetS. The model can be applied to support both clinical practitioners and individuals in clinical and personalized health management systems. The information provided by our proposed model will reduce the financial and emotional burdens related to the presence of MetS. Furthermore, individuals can be motivated by the early knowledge of the risk of MetS to lead a healthier lifestyle and implement preventive measures. Our proposed method is relatively feasible and cost effective in diagnosing MetS because it requires are measurement values from the clinically recognized risk factors-fasting blood glucose, high blood pressure, triglyceride, HDL-Cholesterol and waist circumferences. This renders our proposed method to be easily applicable in both clinical and personalized health care systems.

REFERENCES

[1] G. M. Reaven, "Role of insulin resistance in human disease," *Diabetes*, vol. 37, no. 12, pp. 1595–1607, 1988.
[2] R. M. Parikh and V. Mohan, "Changing definitions of metabolic syndrome," *Indian J. Endocrinol. Metabolism*, vol. 16, no. 1, pp. 7–12, 2012.
[3] S. M. Grundy *et al.*, "Diagnosis and management of the metabolic syndrome," *Amer. Heart Assoc./Nat. Heart, Lung, Blood Inst. Sci. Statement*, vol. 112, no. 17, pp. 2735–2752, 2005.
[4] E. A. García-Villegas, I. Lerman-Garber, L. F. Flores-Suárez, C. Aguilar-Salinas, H. M. González, and A. R. Villa-Romero, "Prognostic value of metabolic syndrome for the development of cardiovascular disease in a cohort of premenopausal women with systemic lupus erythematosus," *Med. Clin.*, vol. 144, no. 7, pp. 289–296, 2015.
[5] S. Demir *et al.*, "Metabolic syndrome is not only a risk factor for cardiovascular diseases in systemic lupus erythematosus but is also associated with cumulative organ damage: A cross-sectional analysis of 311 patients," *Lupus*, vol. 25, no. 2, pp. 177–184, 2016.
[6] C. Lorenzo, M. Okoloise, K. Williams, M. P. Stern, and S. M. Haffner, "The metabolic syndrome as predictor of type 2 diabetes: The San Antonio heart study," *Diabetes Care*, vol. 26, no. 11, pp. 3153–3159, 2003.
[7] S. Brede, G. Serfling, J. Klement, S. M. Schmid, and H. Lehnert, "Clinical scenario of the metabolic syndrome," *Visceral Med.*, vol. 32, no. 5, pp. 336–341, 2016.
[8] N. Peer, C. Lombard, K. Steyn, and N. Levitt, "High prevalence of metabolic syndrome in the Black population of cape town: The Cardiovascular risk in black South Africans (CRIBSA) study," *Eur. J. Preventive Cardiol.*, vol. 22, no. 8, pp. 1036–1042, 2015.
[9] A. Scuteri *et al.*, "Metabolic syndrome across europe: Different clusters of risk factors," *Eur. J. Preventive Cardiol.*, vol. 22, no. 4, pp. 486–491, 2015.
[10] J. R. Banegas *et al.*, "Achievement of lipoprotein goals among patients with metabolic syndrome at high cardiovascular risk across Europe. The EURIKA study," *Int. J. Cardiol.*, vol. 166, no. 1, pp. 210–214, 2013.
[11] E. S. Ford, W. H. Giles, and A. H. Mokdad, "Increasing prevalence of the metabolic syndrome among us adults," *Diabetes Care*, vol. 27, no. 10, pp. 2444–2449, 2004.
[12] B. Trabert, N. Wentzensen, A. S. Felix, H. P. Yang, M. E. Sherman, and L. A. Brinton, "Metabolic syndrome and risk of endometrial cancer in the United States: A study in the SEER–medicare linked database," *Cancer Epidemiol. Biomarkers Prevention*, vol. 24, no. 1, pp. 261–267, 2015.
[13] A. Billow *et al.*, "Prevalence and clinical profile of metabolic syndrome among type 1 diabetes mellitus patients in Southern India," *J. Diabetes Complications*, vol. 29, no. 2, pp. 659–664, 2015.
[14] P. Nestel *et al.*, "Metabolic syndrome: Recent prevalence in East and Southeast Asian populations," *Asia Pacific J. Clin. Nutrition*, vol. 16, no. 2, pp. 362–367, 2007.
[15] W.-H. Pan, W.-T. Yeh, and L.-C. Weng, "Epidemiology of metabolic syndrome in Asia," *Asia Pacific J. Clin. Nutrition*, vol. 17, no. S1, pp. 37–42, 2008.
[16] W. N. W. Mohamud *et al.*, "Prevalence of metabolic syndrome and its risk factors in adult Malaysians: Results of a nationwide survey," *Diabetes Res. Clin. Pract.*, vol. 91, no. 2, pp. 239–245, 2011.
[17] K. S. Heng, A. R. Hejar, A. Z. Rushdan, and S. P. Loh, "Prevalence of metabolic syndrome among staff in a Malaysian public University based on harmonised, international diabetes federation and national cholesterol education program definitions," *Malaysian J. Nutrition*, vol. 19, no. 1, pp. 77–86, 2013.
[18] A. A. Fadzlina *et al.*, "Metabolic syndrome among 13 year old adolescents: Prevalence and risk factors," *BMC Public Health*, vol. 14, no. 3, p. S7, 2014.
[19] W. Aekplakorn, V. Chongsuvivatwong, P. Tatsanavivat, and P. Suriyawongpaisal, "Prevalence of metabolic syndrome defined by the international diabetes federation and national cholesterol education program criteria among thai adults," *Asia Pacific J. Public Health*, vol. 23, no. 5, pp. 792–800, 2011.

[20] W. R. W. Omar, I. Patterson, and S. Pegg, "Healthy lifestyle: Promoting walking behaviourin Kuala Lumpur, Malaysia," *World*, vol. 3, no. 1, pp. 109–123, 2011.

[21] M. Amiri, H. A. Majid, F. M. Hairi, N. Thangiah, A. Bulgiba, and T. T. Su, "Prevalence and determinants of cardiovascular disease risk factors among the residents of urban community housing projects in Malaysia," *BMC Public Health*, vol. 14, no. 3, p. S3, 2014.

[22] F. He *et al.*, "Abdominal obesity and metabolic syndrome burden in adolescents—Penn state children cohort study," *J. Clin. Densitometry*, vol. 18, no. 1, pp. 30–36, 2015.

[23] P. M. Kearney, M. Whelton, K. Reynolds, P. Muntner, P. K. Whelton, and J. He, "Global burden of hypertension: Analysis of worldwide data," *LANCET*, vol. 365, no. 9455, pp. 217–223, 2005.

[24] K. Srikanthan, A. Feyh, H. Visweshwar, J. I. Shapiro, and K. Sodhi, "Systematic review of metabolic syndrome biomarkers: A panel for early detection, management, and risk stratification in the west virginian population," *Internal J. Med. Sci.*, vol. 13, no. 1, pp. 25–38, 2016.

[25] K. G. M. M. Alberti and P. F. Zimmet, "Definition, diagnosis and classification of diabetes mellitus and its complications. Part 1: Diagnosis and classification of diabetes mellitus. provisional report of a WHO consultation," *Diabetic Med.*, vol. 15, no. 2, pp. 539–553, 1998.

[26] Expert Panel on Detection, Evaluation, and Treatment of High Blood Cholesterol in Adults, "Executive summary of the third report of the national cholesterol education program (NCEP) expert panel on detection, evaluation, and treatment of high blood cholesterol in adults (adult treatment panel III)," *JAMA*, vol. 285, no. 19, pp. 2486–2497, 2001, doi: 10.1001/jama.285.19.2486.

[27] G. Alberti, P. Zimmet, J. Shaw, and S. M. Grundy, "The IDF consensus worldwide definition of the metabolic syndrome," Int. Diabetes Fed., Brussels, Belgium, 2006, pp. 1–24. [Online]. Available: https://www.idf.org/e-library/consensus-statements/60-idfconsensus-worldwide-definitionof-the-metabolic-syndrome.html

[28] B. Balkau and M.-A. Charles, "Comment on the provisional report from the WHO consultation. European group for the study of insulin resistance (EGIR)," *Diabetic Med.*, vol. 16, no. 2, pp. 442–443, 1999.

[29] S. M. Grundy *et al.*, "Implications of recent clinical trials for the national cholesterol education program adult treatment panel iii guidelines," *J. Amer. College Cardiol.*, vol. 44, no. 3, pp. 720–732, 2004.

[30] K. Alberti *et al.*, "Harmonizing the metabolic syndrome: A joint interim statement of the international diabetes federation task force on epidemiology and prevention; national heart, lung, and blood Institute; American heart association; world heart federation; international atherosclerosis society; and international association for the study of obesity," *Circulation*, vol. 120, no. 16, pp. 1640–1645, 2009.

[31] E. Shadmi, "Disparities in multiple chronic conditions within populations," *J. Comorbidity*, vol. 3, no. 2, pp. 45–50, 2013.

[32] F. M. Moy and A. Bulgiba, "The modified NCEP ATP III criteria maybe better than the IDF criteria in diagnosing metabolic syndrome among malays in Kuala Lumpur," *BMC Public Health*, vol. 10, no. 1, p. 678, 2010.

[33] H. N. Ginsberg, "Treatment for patients with the metabolic syndrome," *Amer. J. Cardiol.*, vol. 91, no. 7, pp. 29–39, 2003.

[34] L. S. Batey *et al.*, "Summary measures of the insulin resistance syndrome are adverse among Mexican-American versus non-hispanic white children: The corpus christi child heart study," *Circulation*, vol. 96, no. 12, pp. 4319–4325, 1997.

[35] J. C. Eisenmann, "On the use of a continuous metabolic syndrome score in pediatric research," *Cardiovascular Diabetology*, vol. 7, no. 2, p. 17, 2008.

[36] K. Wijndaele *et al.*, "Sedentary behaviour, physical activity and a continuous metabolic syndrome risk score in adults," *Eur. J. Clin. Nutrition*, vol. 63, no. 3, p. 421, 2009.

[37] N. K. Vikram, R. M. Pandey, A. Misra, K. Goel, and N. Gupta, "Factor analysis of the metabolic syndrome components in Urban Asian Indian adolescents," *Asia Pacific J. Clin. Nutrition*, vol. 18, no. 2, pp. 293–300, 2009.

[38] I. S. Okosun, R. Lyn, M. Davis-Smith, M. Eriksen, and P. Seale, "Validity of a continuous metabolic risk score as an index for modeling metabolic syndrome in adolescents," *Ann. Epidemiol.*, vol. 20, no. 11, pp. 843–851, 2010.

[39] K. Mochizuki, R. Miyauchi, Y. Misaki, Y. Ichikawa, and T. Goda, "Principal component 1 score calculated from metabolic syndrome diagnostic parameters is a possible marker for the development of metabolic syndrome in middle-aged Japanese men without treatment for metabolic diseases," *Eur. J. Nutrition*, vol. 52, no. 1, pp. 67–74, 2013.

[40] V. Gaio *et al.*, "Genetic variation at the CYP2C19 gene associated with metabolic syndrome susceptibility in a south portuguese population: Results from the pilot study of the European health examination survey in Portugal," *Diabetol. Metabolic Syndrome*, vol. 6, no. 1, p. 23, 2014.

[41] S. J. Carroll, C. Paquet, N. J. Howard, R. J. Adams, A. W. Taylor, and M. Daniel, "Validation of continuous clinical indices of cardiometabolic risk in a cohort of Australian adults," *BMC Cardiovascular Disorders*, vol. 14, no. 1, p. 27, 2014.

[42] M. J. Gurka, C. L. Lilly, M. N. Oliver, and M. D. DeBoer, "An examination of sex and racial/ethnic differences in the metabolic syndrome among adults: A confirmatory factor analysis and a resulting continuous severity score," *Metabolism*, vol. 63, no. 2, pp. 218–225, 2014.

[43] A. S. Neto, W. de Campos, G. C. Dos Santos, and O. M. Junior, "Metabolic syndrome risk score and time expended in moderate to vigorous physical activity in adolescents," *BMC Pediatrics*, vol. 14, no. 1, p. 42, 2014.

[44] E. Ayubi, D. Khalili, A. Delpisheh, F. Hadaegh, and F. Azizi, "Factor analysis of metabolic syndrome components and predicting type 2 diabetes: Results of 10-year follow-up in a middle eastern population," *J. Diabetes*, vol. 7, no. 6, pp. 830–838. 2015.

[45] R. Heshmat *et al.*, "Is the association of continuous metabolic syndrome risk score with body mass index independent of physical activity? The caspian-III study," *Nutrition Res. Pract.*, vol. 9, no. 4, pp. 404–410, 2015.

[46] J. F. Wiley, M. J. Carrington, "A metabolic syndrome severity score: A tool to quantify cardio-metabolic risk factors," *Preventive Med.*, vol. 88, pp. 189–195, Jul. 2016.

[47] I. T. Jolliffe and J. Cadima, "Principal component analysis: A review and recent developments," *Phil. Trans. R. Soc. A*, vol. 374, p. 20150202, Apr. 2016.

[48] M. J. Gurka *et al.*, "Independent associations between a metabolic syndrome severity score and future diabetes by sex and race: The atherosclerosis risk in communities study and Jackson heart study," *Diabetologia*, vol. 60, no. 7, pp. 1261–1270, 2017.

[49] S. K. Musani, L. J. Martin, J. G. Woo, M. Olivier, M. J. Gurka, and M. D. DeBoer, "Heritability of the severity of the metabolic syndrome in whites and blacks in 3 large cohortsclinical perspective," *Circulat., Genomic Precis. Med.*, vol. 10 no. 2, p. e001621, 2017.

[50] S. Jeong, Y. M. Jo, S.-O. Shim, Y.-J. Choi, and C.-H. Youn, "A novel model for metabolic syndrome risk quantification based on areal similarity degree," *IEEE Trans. Biomed. Eng.*, vol. 61, no. 3, pp. 665–679, Mar. 2014.

[51] I. Soldatovic, R. Vukovic, D. Culafic, M. Gajic, and V. Dimitrijevic-Sreckovic, "siMS score: Simple method for quantifying metabolic syndrome," *PLoS ONE*, vol. 11, no. 1, p. e0146143, 2016.

[52] H. A. Kakudi, C. K. Loo, and K. Pasupa, "Risk quantification of metabolic syndrome with quantum particle swarm optimisation," in *Proc. 26th Int. Conf. World Wide Web Companion, Int. World Wide Web Conf. Steering Committee*, 2017, pp. 1141–1147.

[53] H. A. Kakudi, C. K. Loo, and F. M. Moy, "Predicting metabolic syndrome using risk quantification and ensemble methods," in *Proc. IEEE Symp. Ser. Comput. Intell. (SSCI)*, Nov./Dec. 2017, pp. 1–8.

[54] H. Hirose, T. Takayama, S. Hozawa, T. Hibi, and I. Saito, "Prediction of metabolic syndrome using artificial neural network system based on clinical data including insulin resistance index and serum adiponectin," *Comput. Biol. Med.*, vol. 41, no. 11, pp. 1051–1056, 2011.

[55] Y. Ushida *et al.*, "Combinational risk factors of metabolic syndrome identified by fuzzy neural network analysis of health-check data," *BMC Med. Inform. Decision Making*, vol. 12, no. 1, p. 80, 2012.

[56] M. Murguía-Romero, R. Jiménez-Flores, A. R. Méndez-Cruz, and R. Villalobos-Molina, "Predicting metabolic syndrome with neural networks," in *Proc. Mexican Int. Conf. Artif. Intell. (MICAI)* (Lecture Notes in Computer Science), vol. 8265, F. Castro, A. Gelbukh, and M. González, Eds. Berlin, Germany: Springer, 2013, pp. 464–472.

[57] Y. Zhang, H. Ji, and W. Zhang, "TPPFAM: Use of threshold and posterior probability for category reduction in fuzzy ARTMAP," *Neurocomputing*, vol. 124, pp. 63–71, Jan. 2014.

[58] J. Van Schependom *et al.*, "Do advanced statistical techniques really help in the diagnosis of the metabolic syndrome in patients treated with second-generation antipsychotics?" *J. Clin. Psychiatry*, vol. 76, no. 10, pp. e1292-1–e1292-9, 2015.

[59] M. Romero-Saldaña, F. J. Fuentes-Jiménez, M. Vaquero-Abellán, C. Àlvarez-Fernândez, G. Molina-Recio, and J. López-Miranda, "New non-invasive method for early detection of metabolic syndrome in the working population," *Eur. J. Cardiovascular Nursing*, vol. 15, no. 7, pp. 549–558, 2016.

[60] G. A. Carpenter, S. Grossberg, N. Markuzon, J. H. Reynolds, and D. B. Rosen, "Fuzzy ARTMAP: A neural network architecture for incremental supervised learning of analog multidimensional maps," *IEEE Trans. Neural Netw.*, vol. 3, no. 5, pp. 698–713, Sep. 1992.
[61] B. Vigdor and B. Lerner, "The Bayesian ARTMAP," *IEEE Trans. Neural Netw.*, vol. 18, no. 6, pp. 1628–1644, Nov. 2007.
[62] W. S. Liew, M. Seera, and C. K. Loo, "Hierarchical parallel genetic optimization fuzzy ARTMAP ensemble," *Neural Process. Lett.*, vol. 44, no. 2, pp. 451–470, 2016.
[63] D. Ivanović, A. Kupusinac, E. Stokić, R. Doroslovački, and D. Ivetić, "ANN prediction of metabolic syndrome: A complex puzzle that will be completed," *J. Med. Syst.*, vol. 40, no. 12, p. 264, 2016.
[64] X. Zhao *et al.*, "Application of the back-error propagation artificial neural network (bpann) on genetic variants in the PPAR-γ and RXR-α gene and risk of metabolic syndrome in a chinese han population," *J. Biomed. Res.*, vol. 28, no. 2, p. 114, 2014.
[65] S. Grossberg, "How does a brain build a cognitive code?" *Psychol. Rev.*, vol. 87, no. 1, pp. 1–51, 1980.
[66] G. A. Carpenter, S. Grossberg, and J. H. Reynolds, "ARTMAP: Supervised real-time learning and classification of nonstationary data by a self-organizing neural network," *Neural Netw.*, vol. 4, no. 5, pp. 565–588, 1991.
[67] G. A. Carpenter, S. Grossberg, and D. B. Rosen, "Fuzzy ART: Fast stable learning and categorization of analog patterns by an adaptive resonance system," *Neural Netw.*, vol. 4, no. 6, pp. 759–771, 1991.
[68] A. Koufakou, M. Georgiopoulos, G. Anagnostopoulos, and T. Kasparis, "Cross-validation in fuzzy ARTMAP for large databases," *Neural Netw.*, vol. 14, no. 9, pp. 1279–1291, 2001.
[69] S. Marriott and R. F. Harrison, "A modified fuzzy ARTMAP architecture for the approximation of noisy mappings," *Neural Netw.*, vol. 8, no. 2, pp. 619–641, 1995.
[70] G. A. Carpenter and W. D. Ross, "ART-EMAP: A neural network architecture for object recognition by evidence accumulation," *IEEE Trans. Neural Netw.*, vol. 6, no. 4, pp. 805–818, Jul. 1995.
[71] J. R. Williamson, "Gaussian ARTMAP: A neural network for fast incremental learning of noisy multidimensional maps," *Neural Netw.*, vol. 9, no. 5, pp. 881–897, 1996.
[72] G. A. Carpenter and N. Markuzon, "ARTMAP-IC and medical diagnosis: Instance counting and inconsistent cases," *Neural Netw.*, vol. 11, no. 2, pp. 323–336, 1998.
[73] L. Cervantes, J.-S. Lee, and J. Lee, "Agent-based approach to distributed ensemble learning of fuzzy ARTMAP classifiers," in *Agent and Multi-Agent Systems: Technologies and Applications*, N. T. Nguyen, A. Grzech, R. J. Howlett, and L. C. Jain, Eds. Berlin, Germany: Springer, 2007, pp. 805–814.
[74] E. Granger, P. Henniges, L. S. Oliveira, and R. Sabourin, "Particle swarm optimization of fuzzy ARTMAP parameters," in *Proc. IEEE Int. Joint Conf. Neural Netw.*, Jul. 2006, pp. 2060–2067.
[75] R. Palaniappan and C. Eswaran, "Using genetic algorithm to select the presentation order of training patterns that improves simplified fuzzy ARTMAP classification performance," *Appl. Soft Comput.*, vol. 9, no. 1, pp. 100–106, 2009.
[76] C. K. Loo, W. S. Liew, M. Seera, and E. Lim, "Probabilistic ensemble fuzzy ARTMAP optimization using hierarchical parallel genetic algorithms," *Neural Comput. Appl.*, vol. 26, no. 2, pp. 263–276, 2015.
[77] A. P. Bradley, "The use of the area under the ROC curve in the evaluation of machine learning algorithms," *Pattern Recognit.*, vol. 30, no. 7, pp. 1145–1159, 1997.
[78] D. E. Goldberg and R. Lingle, Jr., "Alleleslociand the traveling salesman problem," in *Proc. 1st Int. Conf. Genetic Algorithms*. Hillsdale, NJ, USA: L. Erlbaum Associates, 1985, pp. 154–159.
[79] F. M. Moy *et al.*, "Cohort study on clustering of lifestyle risk factors and understanding its association with stress on health and wellbeing among school teachers in Malaysia (CLUSTer)—A study protocol," *BMC Public Health*, vol. 14, no. 1, p. 611, 2014.
[80] J. Franklin, "The elements of statistical learning: Data mining, inference and prediction," *Math. Intell.*, vol. 27, no. 2, pp. 83–85, 2005.
[81] M. S. Pepe, *The Statistical Evaluation of Medical Tests for Classification and Prediction*. London, U.K.: Oxford Univ. Press, 2003.
[82] J. A. Swets, "ROC analysis applied to the evaluation of medical imaging techniques," *Investigative Radiol.*, vol. 14, no. 2, pp. 109–121, 1979.
[83] J. H. Friedman, "Greedy function approximation: A gradient boosting machine," *Ann. Statist.*, vol. 29, pp. 1189–1232, 2001.
[84] K. Yamaoka and T. Tango, "Effects of lifestyle modification on metabolic syndrome: A systematic review and meta-analysis," *BMC Med.*, vol. 10, no. 1, p. 138, 2012.
[85] R. Parikh, A. Mathai, S. Parikh, G. C. Sekhar, and R. Thomas, "Understanding and using sensitivity, specificity and predictive values," *Indian J. Ophthalmol.*, vol. 56, no. 1, p. 45, 2008.
[86] J. B. Meigs, D. M. Nathan, J. I. Wolfsdorf, and J. E. Mulder. (2017). *The Metabolic Syndrome (Insulin Resistance Syndrome or Syndrome X)*. [Online]. Available: https://www.uptodate.com/contents/the-metabolic-syndrome-insulin-resistance-syndrome-or-syndrome-x and https://www.uptodate.com/contents/the-metabolic-syndrome-insulin-resistance-syndrome-or-syndrome-x
[87] F. J. Snoek, M. A. Bremmer, and N. Hermanns, "Constructs of depression and distress in diabetes: Time for an appraisal," *Lancet Diabetes Endocrinol.*, vol. 3, no. 6, pp. 450–460, 2015.
[88] M. X. Hu, F. Lamers, S. A. Hiles, B. W. J. H. Penninx, and E. J. C. de Geus, "Basal autonomic activity, stress reactivity, and increases in metabolic syndrome components over time," *Psychoneuroendocrinology*, vol. 71, pp. 119–126, Sep. 2016.
[89] F. Bonomini, L. F. Rodella, and R. Rezzani, "Metabolic syndrome, aging and involvement of oxidative stress," *Aging Disease*, vol. 6, no. 2, p. 109, 2015.
[90] W. H. Dietz *et al.*, "Management of obesity: Improvement of healthcare training and systems for prevention and care," *LANCET*, vol. 385, no. 9986, pp. 2521–2533, 2015.
[91] P. Chu, R. A. Gotink, G. Y. Yeh, S. J. Goldie, and M. G. Hunink, "The effectiveness of yoga in modifying risk factors for cardiovascular disease and metabolic syndrome: A systematic review and meta-analysis of randomized controlled trials," *Eur. J. Preventive Cardiol.*, vol. 23, no. 2, pp. 291–307, 2016.

HABEEBAH ADAMU KAKUDI received the B.Tech. degree in mathematics and computer science from the Federal University of Technology, Minna, Nigeria, in 1998, and the M.Sc. degree in computer science from Bayero University, Kano, Nigeria, in 2011.

She is currently pursuing the Ph.D. degree with the University of Malaya and a Lecturer with Bayero University. Her current research interests include disease prediction, soft computing, evolutionary computing, machine learning, and automated healthcare systems.

CHU KIONG LOO (SM'14) received the B.Eng. degree (Hons.) in mechanical engineering from the University of Malaya, Kuala Lumpur, Malaysia, and the Ph.D. degree from Universiti Sains Malaysia, George Town, Malaysia. He was a Design Engineer with various industrial firms and is the Founder of the Advanced Robotics Laboratory, University of Malaya. He has been involved in the application of research into Peruss quantum associative model and Pribram's holonomic brain model in humanoid vision projects. He is currently a Professor of computer science and information technology with the University of Malaya.

He has led many projects funded by the Ministry of Science in Malaysia and the High Impact Research Grant from the Ministry of Higher Education, Malaysia. His current research interests include brain-inspired quantum neural networks, constructivism-inspired neural networks, synergetic neural networks, and humanoid research.

FOONG MING MOY received the master's degrees in public health and nutrition and the Ph.D. degree in public health from the University of Malaya. She is currently a Nutritional Epidemiologist from the Epidemiology and Biostatistics Unit, Department of Social and Preventive Medicine, Faculty of Medicine, University of Malaya, Kuala Lumpur. She is a Dietitian by profession. Her research interests include translational research in the prevention of non-communicable diseases (NCDs) in the community setting, workplace wellness, and the effects of lifestyle behaviors on NCDs. Her latest project is on the promotion of sustainable diets in collaboration with NGOs, such as WWF-Malaysia and Health Promotion Board Malaysia.

NAOKI MASUYAMA (S'12–M'16) received the B.Eng. degree from Nihon University, Tokyo, Japan, in 2010, the M.Eng. degree from Tokyo Metropolitan University, Tokyo, in 2012, and the Ph.D. degree from the Faculty of Computer Science and Information Technology, University of Malaya, Kuala Lumpur, Malaysia, in 2016. He is currently an Assistant Professor with the Department of Computer Science and Intelligent Systems, Graduate School of Engineering, Osaka Prefecture University. His current research interests include associative memory, clustering/classification, and human–robot interaction.

KITSUCHART PASUPA (M'12–SM'16) received the B.Eng. degree in electrical engineering from the Sirindhorn International Institute of Technology, Thammasat University, Thailand, in 2003, and the M.Sc. (Eng.) and Ph.D. degrees in automatic control and systems engineering from the Department of Automatic Control and Systems Engineering, The University of Sheffield, in 2004 and 2008, respectively. He was a Research Fellow with the University of Southampton and The University of Sheffield. He is currently an Associate Processor with the Faculty of Information Technology, King Mongkut's Institute of Technology Ladkrabang, Bangkok, Thailand. His main research interests lie in the application of machine learning techniques in the real-world application.